New 24-Pulse Diode Rectifier Systems for Utility Interface of High-Power AC Motor Drives

Sewan Choi, *Member, IEEE*, Bang Sup Lee, *Student Member, IEEE*, and Prasad N. Enjeti, *Senior Member, IEEE*

***Abstract*—This paper proposes two new passive 24-pulse diode rectifier systems for utility interface of pulsewidth modulated (PWM) ac motor drives. The first approach employs an extended delta transformer arrangement, which results in near equal leakage inductance in series with each diode rectifier bridge. This promotes equal current sharing and improved performance. A specially tapped interphase transformer is then introduced with two additional diodes to extend the conventional 12-pulse operation to 24-pulse operation from the input current point of view. The proposed system exhibits clean power characteristics with fifth, seventh, eleventh, thirteenth, seventeenth, and nineteenth harmonics eliminated from the utility line currents. The second scheme is a reduced voltampere approach employing autotransformers to obtain 24-pulse operation. The voltampere rating of the polyphase transformer in the second scheme is $0.23P_o$ (PU). Detailed analysis and simulations verify the proposed concept, and experimental results from a 208-V 10-kVA rectifier system are provided.**

***Index Terms*—AC motor drives, clean power, 24-pulse, utility interface.**

I. Introduction

A number of methods have been proposed to lower harmonics generated by diode rectifier-type utility interfaces to power electronics systems [2]–[6]. One approach is to use a conventional 12-pulse converter which requires two six-pulse converters connected through Δ–Y and Δ–Δ isolation transformers (Fig. 1). An interphase transformer (IPT) is required to ensure independent operation of the two three-phase diode bridge rectifiers. The operation of the conventional 12-pulse converter results in the absence of the fifth and seventh harmonics in the input utility line current. However, the total harmonic distortion (THD) of input line currents are still high and do not qualify as clean power.

In this paper, to further increase the pulse number and cancel several lower order harmonics, a specially tapped interphase transformer is introduced with two additional diodes connected (scheme 1), as shown in Fig. 2. The taps on the interphase transformer are chosen such that 24-pulse characteristics, with the elimination of fifth, seventh, eleventh, thirteenth, seventeenth, and nineteenth harmonics in the input line currents occur. Thus, the proposed approach extends the conventional 12-pulse operation to 24-pulse operation from the input current point of view, with slight complexity in hardware. Further, a reduced voltampere 24-pulse system employing an autotransformer configuration is introduced (scheme 2), as shown in Fig. 6. The voltampere rating of the polyphase transformer in the second scheme is $0.23P_o$ (PU), which drastically reduces the cost, weight, and volume. Both schemes 1 and 2 exhibit clean power characteristics and are considered as important contributions.

Detailed analysis of the tapped interphase transformer design and the resulting 24-pulse diode rectifier system are discussed. The proposed systems are simulated on SABER and experimental results from a 208-V 10-kVA laboratory system are also provided.

Paper IPCSD 96–59, approved by the Industrial Power Converter Committee of the IEEE Industry Applications Society for presentation at the 1996 IEEE Applied Power Electronics Conference and Exposition, San Jose, CA, March 3–7. Manuscript released for publication November 11, 1996.

S. Choi was with the Power Electronics Laboratory, Research and Development Center, Samsung Electro-Mechanics Company, Ltd., Suwon, 442-743 Korea. He is now with the Department of Control and Instrumentation, Seoul National Polytechnical University, Seoul, Korea.

B. S. Lee is with the Department of Electrical Engineering, Texas A&M University, College Station, TX 77843-3128 USA (e-mail: banglee@ee.tamu.edu).

P. N. Enjeti is with the Department of Electrical Engineering, Texas A&M University, College Station, TX 77843 USA (e-mail: p.enjeti@ieee.org).

Publisher Item Identifier S 0093-9994(97)01764-7.

II. Proposed 24-Pulse Approach (Scheme 1)

Fig. 2 shows the proposed 24-pulse system, which is identical to the conventional 12-pulse system, with the exception of a modified transformer configuration and the two diodes connected to a specially tapped interphase transformer. The secondary windings of the input transformer are configured in extended delta and generate balanced sets of three-phase voltages with 30° phase shift for the diode rectifiers. The extended delta arrangement provides equal leakage reactances in series with rectifiers I and II. More details on transformer winding arrangements are discussed in Section II-B.

A. Operation of the Tapped-Interphase Transformer

The tapped-interphase transformer has been discussed in [2] for SCR converters with multiple taps, along with a complicated firing scheme. In this paper, it is shown that by employing only two taps and two additional diodes, conventional 12-pulse operation can be extended to 24-pulse operation with the fifth, seventh, eleventh, thirteenth, seventeenth, and nineteenth harmonics eliminated in the input line currents. The resulting system exhibits high performance with clean power characteristics. Fig. 3 shows the practical winding configuration of the two diodes tapped on the interphase transformer and the operation of the interphase transformer according to two modes: P-mode [Fig. 3(a)] and Q-mode [Fig. 3(b)]. Fig. 10(g) shows the voltage waveform across the interphase transformer. Whenever the voltage across the interphase transformer goes positive $(V_m > 0)$, diode D_p is forward-biased and is turned on, D_q is reverse-biased and is

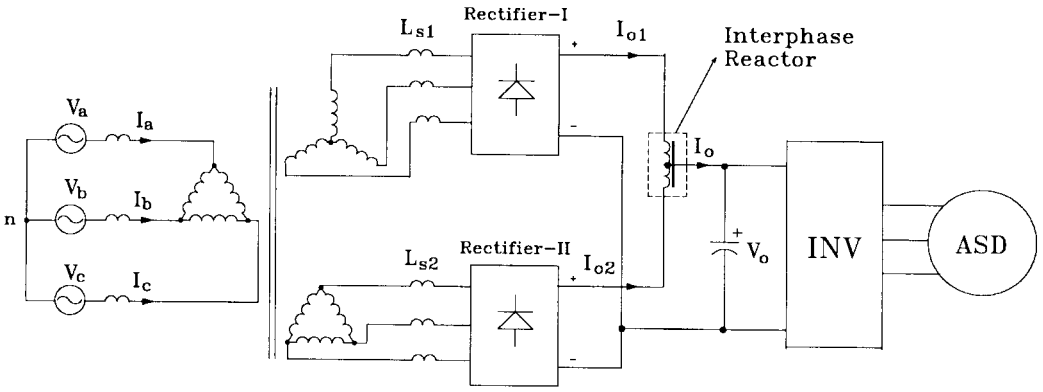

Fig. 1. Conventional 12-pulse system.

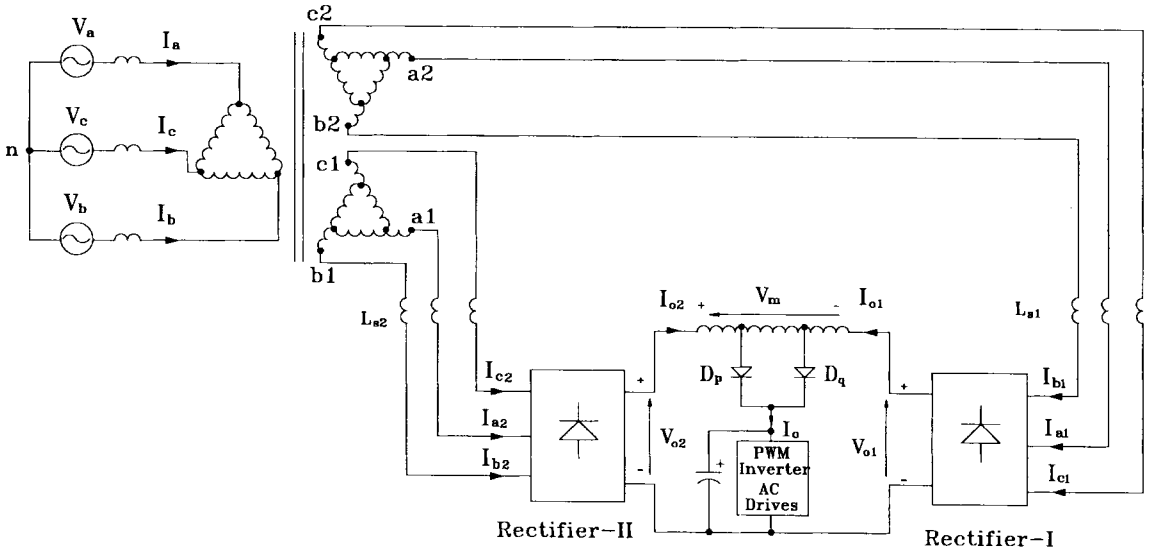

Fig. 2. Proposed 24-pulse system (scheme 1).

off (P-mode), therefore, diode D_p carries load current I_o. The MMF relationship of the interphase transformer for the P-mode is

$$I_{o2}(0.5N_o - N_t) = I_{o1}(0.5N_o + N_t) \quad (1)$$

$$I_{o1} + I_{o2} = I_o \quad (2)$$

where N_o is the total number of turns of the interphase transformer and N_t is the number of turns between the midpoint and the tapped points of the interphase transformer [see Fig. 3(a)]. From (1) and (2), the output currents of the two diode bridge rectifiers are given by

$$I_{o1} = (0.5 - k)I_o \quad (3)$$

$$I_{o2} = (0.5 + k)I_o \quad (4)$$

where $k = N_t/N_o$ and $k = 0$ signify the conventional center-tapped interphase transformer and 12-pulse operation. When voltage across the interphase transformer V_m is negative, diode D_q is forward-biased and is turned on and D_p is reverse-biased and is off, therefore, diode D_q carries load current I_o (Q-mode). Similarly, for Q-mode the output currents of the two diode bridge rectifiers become

$$I_{o1} = (0.5 + k)I_o \quad (5)$$

$$I_{o2} = (0.5 - k)I_o. \quad (6)$$

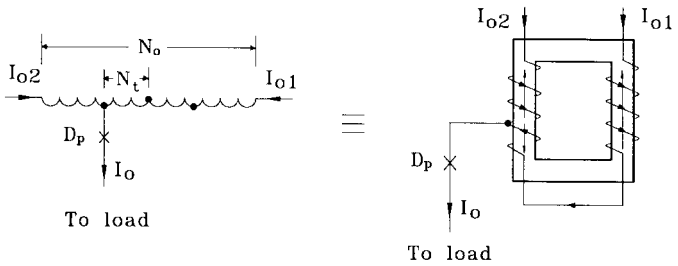

(a)

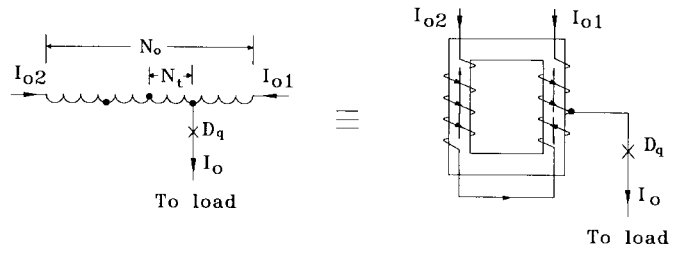

(b)

Fig. 3. Operation of the interphase reactor with two tapped diodes. (a) P-mode. (b) Q-mode.

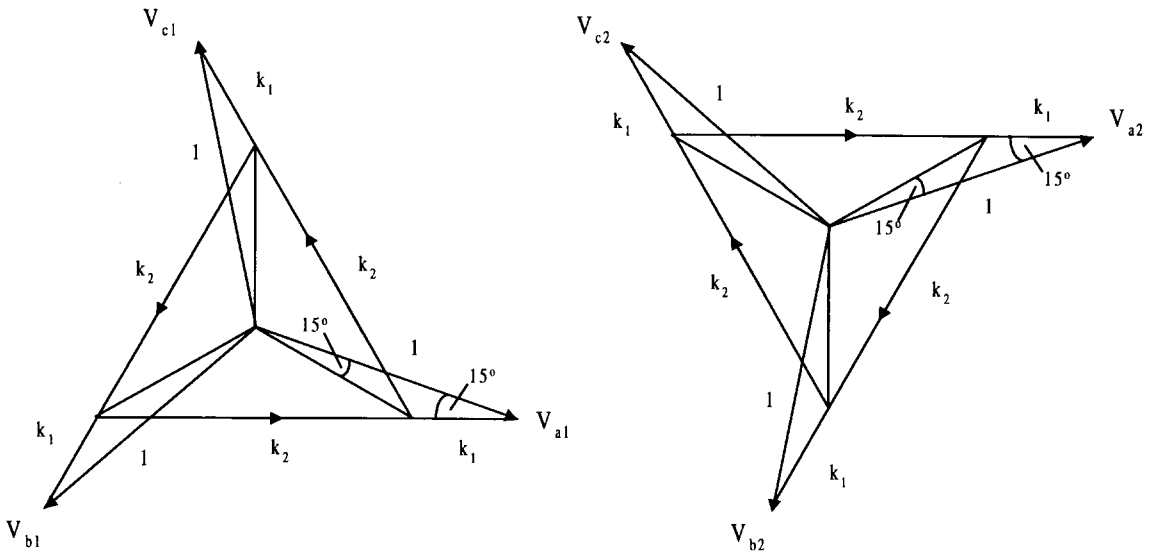

Fig. 4. Vector diagram of the extended delta transformer.

Therefore, depending on the polarity of voltage V_m, the magnitudes of rectifier output currents I_{o1} and I_{o2} are modulated as shown in Fig. 10(d) and (e), and this changes the shapes of rectifier input currents, as shown in Fig. 10(c). Finally, the rectifier system exhibits 24-pulse characteristics, as shown in Fig. 10(a). The next sections describe details of the analysis of input currents and the selection of k, required for 24-pulse operation.

B. Extended Delta Transformer Arrangement

Fig. 2 shows the proposed scheme 1. For scheme 1 to operate successfully as a 24-pulse system, the two-diode rectifier bridges should be balanced and rectifier output currents I_{o1} and I_{o2} be more or less equal in magnitude. In order to achieve this, the input transformer leakage reactances in the secondary winding should be nearly equal. The conventional 12-pulse Δ–Y transformer shown in Fig. 1 suffers from unequal secondary turns, and this contributes to inequality in leakage reactances for the two-diode bridge rectifiers. In order to overcome the limitation, an extended delta transformer is presented in scheme 1.

The vector diagram of the extended delta transformer arrangement for rectifiers I and II in Fig. 2 is shown in Fig. 4. The required phase-shift angle between the two sets of three-phase voltages is 30° to obtain 12-pulse operation. The extended delta arrangement shown in Figs. 4 and 5 presents equal numbers of turns in the secondary windings, hence, near equal leakage reactances in each line of the transformer secondary. This, in turn, ensures equal loading of the two rectifier bridges, resulting in I_{o1} and I_{o2} being equal. Assuming that the magnitude of the line-to-neutral voltages of the secondary winding, such as V_{a1}, is 1 (PU), the extended length k_1 can be obtained from the geometric relationship of

$$\frac{\sin 150^\circ}{1} = \frac{\sin 15^\circ}{k_1} \tag{7}$$

and, therefore,

$$k_1 = 0.5176 \text{ (PU)}. \tag{8}$$

Then, length k_2 for the secondary delta winding can be obtained by

$$k_2 = \sqrt{3}k_1 = 0.8966 \text{ (PU)}. \tag{9}$$

Fig. 5 shows the winding configuration on a three-limb core. From limb A of the three-limb core, the MMF equation becomes

$$\sqrt{3}I_1 = k_1(I_{a1} + I_{a2}) + \frac{1}{3}k_2(I_{a1} - I_{c1} + I_{a2} - I_{b2}). \tag{10}$$

Similarly, for core limbs B and C, the MMF equations become

$$\sqrt{3}I_2 = k_1(I_{b1} + I_{b2}) + \frac{1}{3}k_2(I_{b1} - I_{a1} + I_{b2} - I_{c2})$$
$$\sqrt{3}I_3 = k_1(I_{c1} + I_{c2}) + \frac{1}{3}k_2(I_{c1} - I_{b1} + I_{c2} - I_{a2}). \tag{11}$$

Then, from (10) and (11), input line current I_a can be obtained by

$$I_a = k_1\left(I_{a2} - I_{c1} + \frac{1}{\sqrt{3}}(I_{a1} - I_{c1} + I_{a2} - I_{c2})\right). \tag{12}$$

C. Voltampere Rating of the Extended Delta Transformer and Design Example

The extended delta transformer utilized in the proposed approach is designed and the voltampere rating is calculated in this section. Assuming output power $P_o = 10$ kVA and input line-to-line rms voltage $V_{LL} = 208$ V, output voltage V_o of the proposed rectifier system becomes

$$V_o = 1.35V_{LL} = 280.8 \text{ V}. \tag{13}$$

Output current I_o becomes

$$I_o = \frac{P_o}{V_o} = 35.6 \text{ A}. \tag{14}$$

Assuming that output current I_o has negligible ripple, the rms values of each of the winding voltages and currents can be obtained and listed as in Table I.

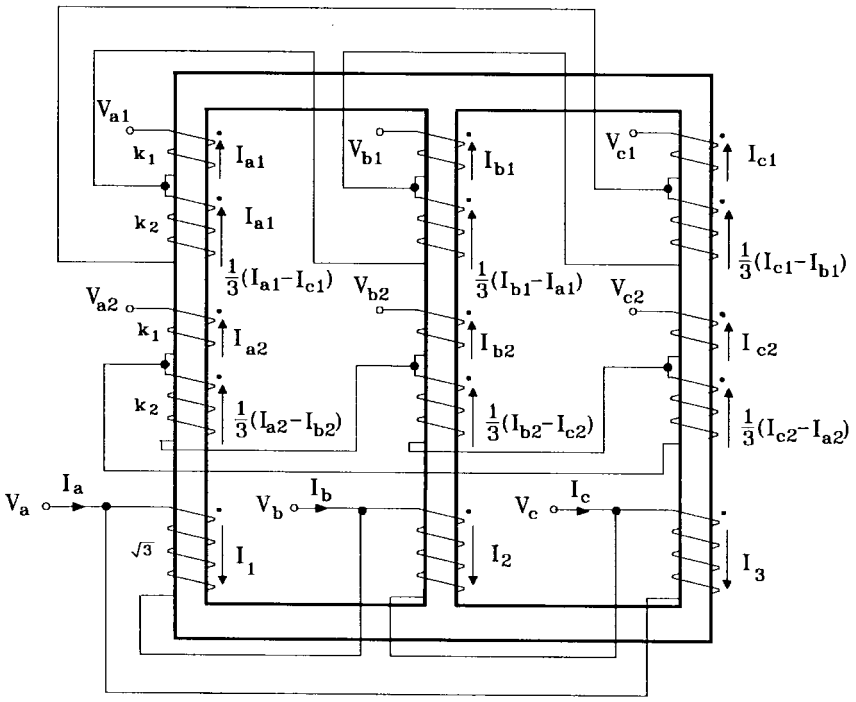

Fig. 5. Winding configuration of the extended delta transformer on a three-limb core.

TABLE I
WINDING VOLTAGES AND CURRENTS OF THE EXTENDED DELTA TRANSFORMER

		Rms. Expression	Rms. Value
Primary winding current	$\lvert I_1 \rvert$	$0.4553\ I_o$	16.21 A
Primary winding voltage	$\lvert V_{ab} \rvert$	$\sqrt{3}\,V_{LN}$	207.85 V
Secondary delta winding current	$\frac{1}{3}\lvert I_{a1} - I_{c1} \rvert$	$0.2357\ I_o$	8.39 A
Secondary delta winding voltage	$\lvert V_{k2} \rvert$	$\sqrt{3}\,k_1\,V_{LN}$	107.58 V
Secondary extended winding current	$\lvert I_{a1} \rvert$	$0.4082\ I_o$	14.54 A
Secondary extended winding voltage	$\lvert V_{k1} \rvert$	$k_1\,V_{LN}$	62.11 V

Then, the total voltamperes of the extended delta transformer becomes

$$\begin{aligned}\mathrm{kVA_{tot}} &= 3 \cdot |I_1| \cdot |V_{ab}| + 6 \cdot \frac{1}{3} \cdot |I_{a1} - I_{c1}| \cdot |V_{k2}| \\ &\quad + 6 \cdot |I_{a1}| \cdot |V_{k1}| \\ &= 20.94\ (\mathrm{kVA}). \end{aligned} \tag{15}$$

Hence, the equivalent voltampere rating of the extended delta transformer is

$$\begin{aligned}\mathrm{kVA_{eq}} &= \frac{1}{2}\mathrm{kVA_{tot}} \\ &= 10.47\ (\mathrm{kVA}) \end{aligned} \tag{16}$$

This illustrates that the required transformer voltamperes for the proposed scheme is almost the same as the conventional delta-wye transformer voltamperes of 10.35 kVA [9].

D. Input Line Current of the Proposed Approach

In this section, the input line currents are analyzed and the interphase transformer tapping ratio k is selected so that the proposed scheme performs as a 24-pulse system from the input current point of view.

From the rectifier input current I_{a1} of Fig. 10(c), it can be seen that the waveforms have half-wave and quarter-wave symmetry. Therefore, the Fourier series of the rectifier input current, I_{a1} shown in Fig. 10(c), can be represented as a function of k as follows:

$$I_{a1}(t) = \sum_{\substack{n=\text{odd},\\ \text{non-triplen}}}^{\infty} b_n(k) \sin(n\omega t). \tag{17}$$

Since the waveform of each input current is identical except for a 120° phase difference,

$$I_{c1}(t) = \sum_{\substack{n=\text{odd},\\ \text{non-triplen}}}^{\infty} b_n(k) \sin(n(\omega t + 120)) \tag{18}$$

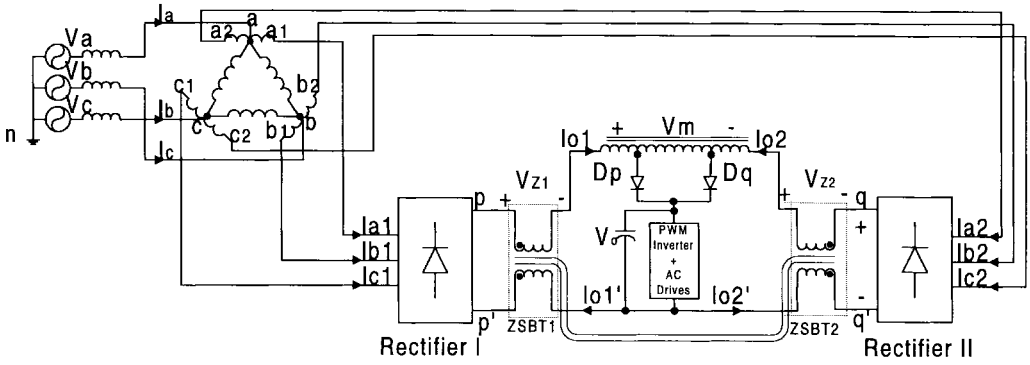

(a)

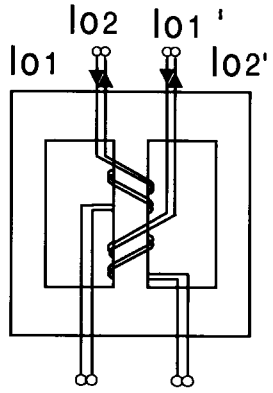

(b)

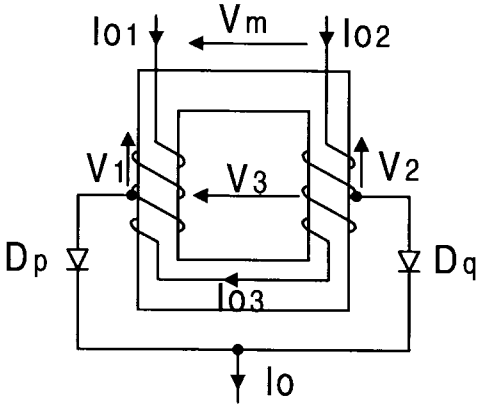

(c)

Fig. 6. Proposed 24-pulse system (scheme 2). (a) Circuit diagram. (b) Shell-type zero-sequence blocking transformer (ZSBT). (c) Winding configuration of the interphase transformer.

$$I_{a2}(t) = \sum_{\substack{n=\text{odd},\\ \text{non-triplen}}}^{\infty} b_n(k)\sin(n(\omega t - 30)) \tag{19}$$

$$I_{c2}(t) = \sum_{\substack{n=\text{odd},\\ \text{non-triplen}}}^{\infty} b_n(k)\sin(n(\omega t + 90)). \tag{20}$$

Then, from (12) and (17)–(20), input line current $I_a(t)$ becomes

$$I_a(t) = \sum_{\substack{n=\text{odd},\\ \text{non-triplen}}}^{\infty} b_n(k) g_n \sin(n\omega t + \phi_n) \tag{21}$$

where $b_n(k), g_n$ and ϕ_n are given by (22), at the bottom of the page. From (22) $g_n = 0$ for $n = 5, 7, 17, 19, 29, 31$, etc. (i.e., $n = 6m \pm 1, m = 1, 3, 5$, etc.) and the value of k for $b_n(k) = 0$ for $n = 11$ and 13 can be found to be

$$k = \frac{N_t}{N_o} = 0.2457. \tag{23}$$

Therefore, substituting the value of k in (23) into (22) results in the elimination of the fifth, seventh, eleventh, thirteenth, seventeenth, and nineteenth harmonics in the input line current I_a, yielding 24-pulse characteristics from the input current standpoint.

III. Proposed 24-Pulse Approach (Scheme 2)

Fig. 6(a) shows a reduced-voltampere approach to the proposed 24-pulse system. This approach employs a polyphase autotransformer to provide 30° phase-shifted voltages to rectifier bridges I and II. The voltamperes transmitted by the actual magnetic coupling is only a portion of the total voltamperes

$$b_n(k) = \frac{4}{n\pi}\left\{(0.5-k)\left(\cos\frac{n\pi}{12} - \cos\frac{5n\pi}{12}\right) + 2k\left(\cos\frac{n\pi}{6} - \cos\frac{n\pi}{3}\right)\right\}$$

$$g_n = \sqrt{\left[\cos\left(\frac{n\pi}{6}\right) + \frac{2}{\sqrt{3}}\sin^2\left(\frac{n\pi}{3}\right)\right]^2 + \left[\sin\left(\frac{n\pi}{6}\right) + \frac{2}{\sqrt{3}}\sin\left(\frac{n\pi}{3}\right)\cos\left(\frac{n\pi}{3}\right)\right]^2}$$

$$\phi_n = \tan^{-1}\left(\frac{-\sin\left(\frac{n\pi}{6}\right) - \frac{2}{\sqrt{3}}\sin\left(\frac{n\pi}{3}\right)\cos\left(\frac{n\pi}{3}\right)}{\cos\left(\frac{n\pi}{6}\right) + \frac{2}{\sqrt{3}}\sin^2\left(\frac{n\pi}{3}\right)}\right) \tag{22}$$

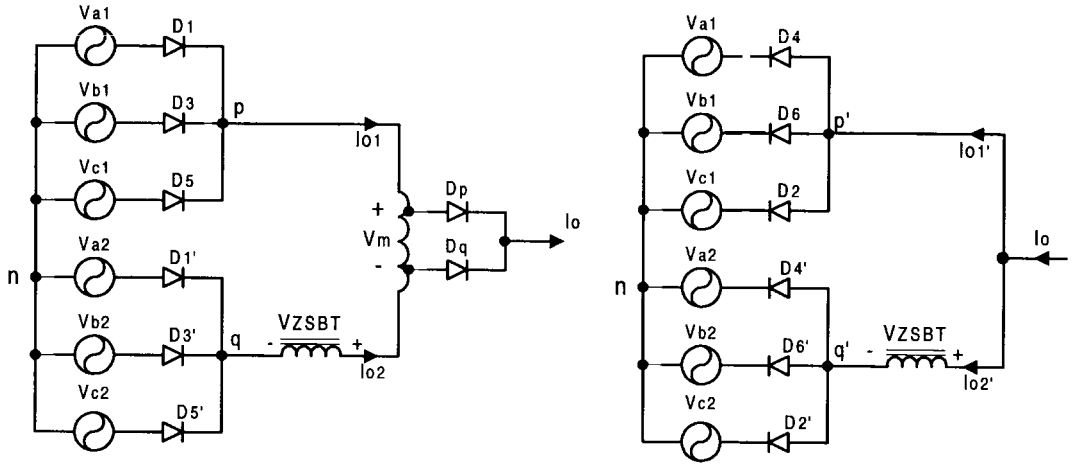

Fig. 7. Equivalent circuit of proposed 24-pulsesystem with ZSBT in dc link. (a) Top group of rectifiers I and II. (b) Bottom group of rectifiers I and II.

and is shown to be $0.23P_o$ (PU). This results in 77% reduction in size of the phase-shifting transformer compared to scheme 1.

To ensure independent operation of the two-diode bridge rectifiers with input autotransformer, a zero-sequence blocking transformer (ZSBT) becomes necessary [9] and is shown in Fig. 6(b). The ZSBT exhibits high impedance to zero-sequence currents and promotes 120° conduction for each rectifier diode. It should be noted that ZSBT's are placed symmetrically in the dc link, which results in equal current sharing in output. The next few sections detail the operating of ZSBT, voltage analysis, and voltampere calculation. Now, with the use of the specially tapped interphase transformer described in Section II-A, the proposed scheme 2 in Fig. 6 also exhibits 24-pulse characteristics. The value of k, tap ratio of the interphase transformer, and input current expression for I_a are identical to scheme 1. Thus, scheme 2 ensures the elimination of the fifth, seventh, eleventh, thirteenth, seventeenth, and nineteenth harmonics in the input line currents. It should be noted that scheme 2 employs reduced voltampere components contributing to lower cost, weight, and volume, as well as having equal current sharing in output. The next few sections detail the operation and function of each component of the proposed 24-pulse system.

A. Zero-Sequence Blocking Transformer (ZSBT)

The ZSBT exhibits significant impedance for zero-sequence current components, thereby eliminating unwanted conduction sequence of the rectifier diodes in an autoconnected system. With a properly designed ZSBT, each rectifier bridge (I and II) operates independently with 120° conduction of each diode in an autoconnected system [10].

1) Voltage Analysis with ZSBT: For the purpose of detailed voltage analysis, an equivalent circuit of the proposed 24-pulse system in Fig. 6(a) is developed and is shown in Fig. 7. The equivalent circuit consists of two positive and negative groups of diodes, as shown in Fig. 7(a) and (b).

In the top group, the cathodes of the diodes 1, 3, and 5 are at a common potential, V_p. Therefore, the diode with its anode at the highest potential will conduct the current I_{o1}. The cathodes of the diodes 1′, 3′, and 5′ are at a common potential, V_q [Fig. 7(a)]. Therefore, the diode with its anode at the highest potential will conduct the current I_{o2} and the rest of the diodes are reverse-biased. Similarly, in the bottom group [Fig. 7 (b)], the diodes with their cathodes at the lowest potential will conduct, and the rest of the diodes are reverse biased. Thus, the voltage across the ZSBT depends on the conduction sequence of diodes. Fig. 8 shows the instantaneous waveshapes of voltages V_p, V_q, V_p', V_q', and V_m due to the conduction of positive and negative groups of diodes, as shown in Fig. 7(a) and (b). Now, from Fig. 7(a) and (b) we have

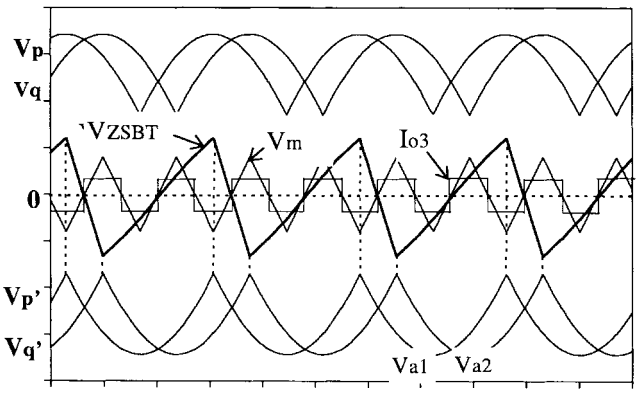

Fig. 8. Voltage across the ZSBT and voltage across the interphase transformer.

$$V_{\text{ZSBT}} = (V_p - V_q) - V_m \tag{24}$$

$$= \begin{cases} V_{a1} - V_{a2} & \text{for } \frac{8}{12}T \sim \frac{11}{12}T \\ V_{b1} - V_{a2} & \text{for } \frac{11}{12}T \sim T \end{cases} \tag{25}$$

where V_{ZSBT} is the voltage across the two ZSBT's in the circuit and T is one period of V_{a1}.

Fig. 8 shows the plot of V_{ZSBT} computed from [(24), (25)] the instantaneous voltages generated due to the conduction of diodes. Mathematically, V_{ZSBT} can be expressed in Fourier

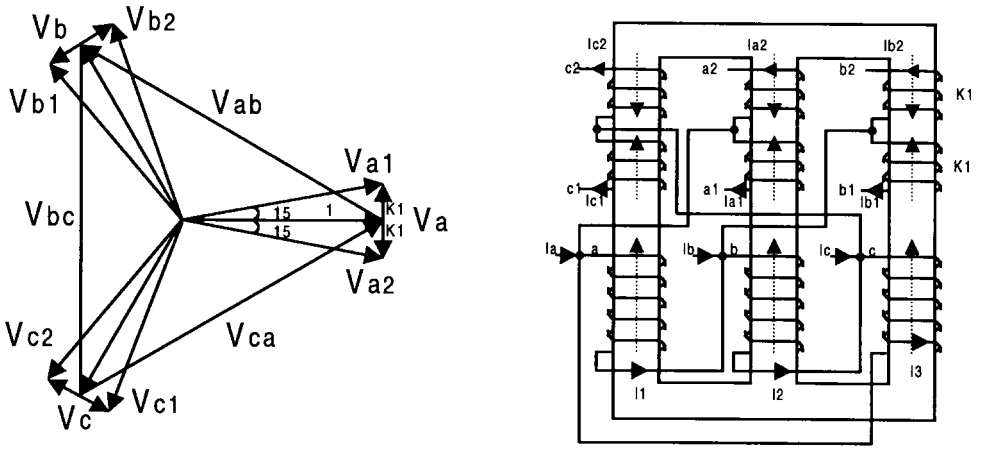

(a) (b)

Fig. 9. Reduced voltampere delta-type polyphase transformer for 24-pulse system. (a) Vector diagram. (b) Winding configuration.

series as

$$V_{\mathrm{ZSBT}}(wt) = V_{LL}(-0.25\cos(3wt) + 0.07\sin(6wt) + 0.03\cos(9wt) + \cdots). \quad (26)$$

It should be noted that V_{ZSBT} contains only tripplen frequency components, hence, if properly designed, it impedes the flow of tripplen harmonic currents or, in other words, ensures independent six-pulse operation of the two rectifier bridges I and II. The average dc output voltage V_o [Fig. 6 (a)] is given by [9]

$$V_{o,\mathrm{av}} = \frac{3\sqrt{2}}{\pi}V_{LL} \times \frac{1}{\cos(15^\circ)} = 1.398V_{LL} \quad (27)$$

where V_{LL} is the rms of the line to line utility voltage. The $V_{o,\mathrm{av}}$ is about 3.5% higher than a conventional six-pulse system.

2) Voltampere Rating of the ZSBT: To compute the voltampere rating of the ZSBT, the rms voltage and rms current magnitudes are necessary. The voltage across the ZSBT [(25)] is plotted in Fig. 8. Also, Fig. 10(d) shows the current I_{o1} carried by the ZSBT winding. The voltampere rating of the ZSBT can be calculated as follows:

$$\mathrm{VA}_{\mathrm{ZSBT}} = V_{\mathrm{ZSBT,rms}} \times I_{o1,\mathrm{rms}}. \quad (28)$$

From (26), we have the rms voltage across the ZSBT as follows:

$$V_{\mathrm{ZSBT,rms}} = 0.185V_{LL}. \quad (29)$$

The rms current through the ZSBT as shown in Fig. 10(d) is given by

$$I_{o1,\mathrm{rms}} = 0.567I_o. \quad (30)$$

Therefore, from (27) to (30), the voltampere rating of the ZSBT is

$$\mathrm{VA}_{\mathrm{ZSBT}} = 0.185V_{LL} \times 0.567I_o = 0.075P_o \quad (31)$$

where P_o is the output power $(V_o \times I_o)$.

It should be noted that the voltampere rating of the ZSBT is small. Further, the lowest frequency component of the voltage across the ZSBT is 180 Hz. This results in small size, weight, and volume.

B. Polyphase Autotransformer

The vector diagram of the proposed delta-type autotransformer connection and the winding configuration on a three-limb core are shown in Fig. 9(a) and (b), respectively. The necessary phase-shift angle between a_1, b_1, c_1 and a_2, b_2, c_2 is 30°. Therefore, from Fig. 9(a) the length k_1 becomes

$$k_1 = \tan(15^\circ) = 0.2679\ [\mathrm{pu}] \quad (32)$$

and the input current I_a from the MMF equations is as follows [9]:

$$I_a = I_{a1} + I_{a2} + \frac{k_1}{\sqrt{3}}(I_{c2} - I_{b2} + I_{b1} - I_{c1}). \quad (33)$$

1) Voltampere Ratings of the Autotransformer and Interphase Transformer: The rms value of the current through the winding with k_1 length [Fig. 10(c)] is

$$I_{a1} = 0.4548I_o. \quad (34)$$

The current $I_{b1}, I_{c1}, I_{a2}, I_{b2}$, and I_{c2} have the same rms value as I_{a1} given in (34). The delta connected winding [Fig. 9(b)] current can be expressed as [9]

$$\sqrt{3}I_1 = k_1(I_{c2} - I_{c1}). \quad (35)$$

Therefore, from (34) and (35), we have

$$I_1 = 0.0775I_o. \quad (36)$$

The rms voltage of the winding with k_1 length is

$$V_{a,a1} = k_1\frac{V_a}{\sqrt{2}} = 0.1107V_o. \quad (37)$$

The rms voltage of the delta connected winding is

$$V_{ab} = \sqrt{\frac{3}{2}}V_a = 0.7157V_o. \quad (38)$$

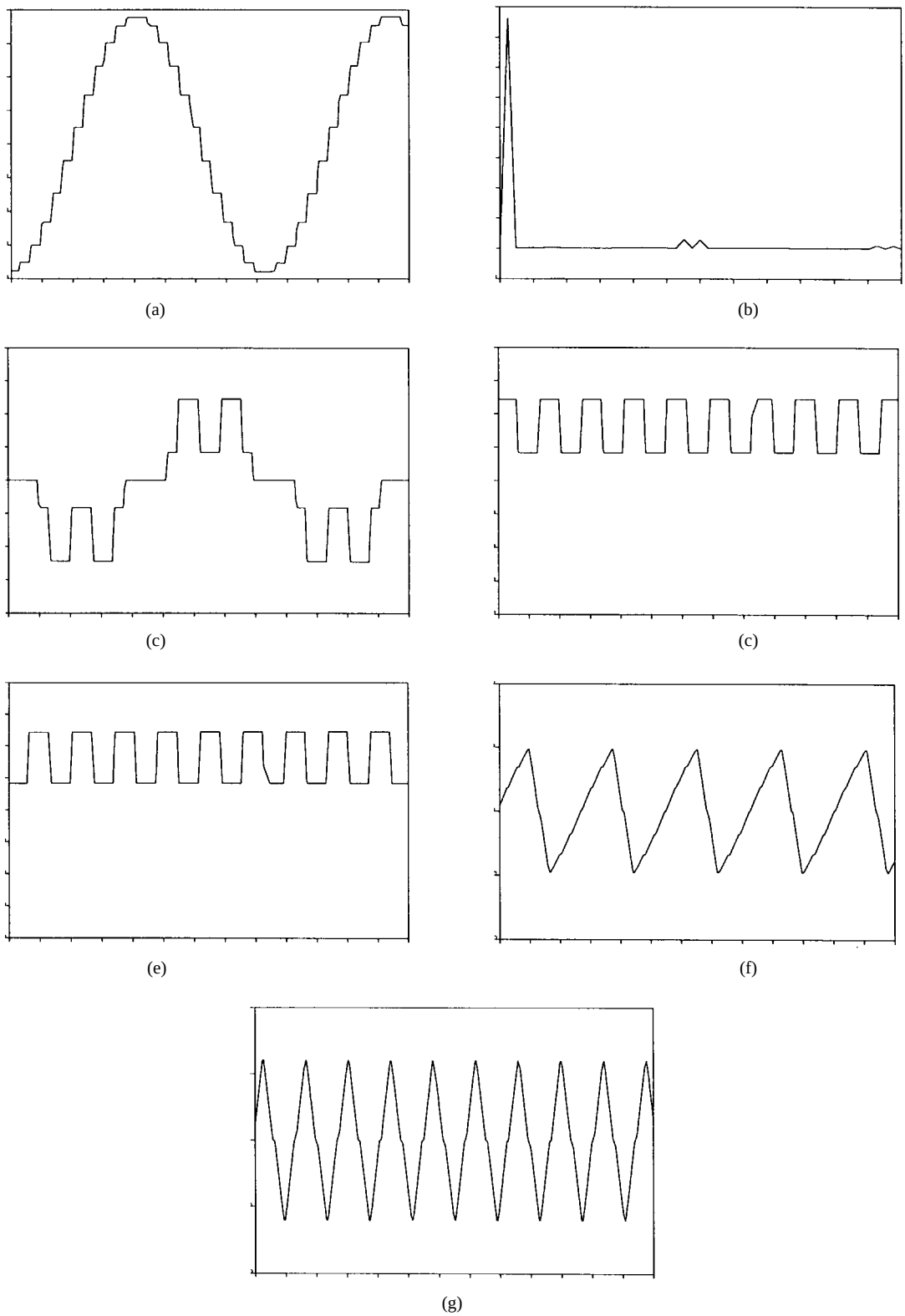

Fig. 10. Simulation results of the proposed system. (a) Input line current I_a. (b) Frequency spectrum of I_a. (c) Rectifier input current I_{a1}. (d) Rectifier output current I_{o1}. (e) Rectifier output current I_{o2}. (f) Voltage across the ZSBT. (g) Voltage across the interphase transformer V_m.

Thus, from (34)–(38), the equivalent voltampere rating of the polyphase transformer is given by

$$\mathrm{VA_{TR}} = \frac{6 \times I_{a1} \times V_{a,a1} + 3 \times I_1 \times V_{ab}}{2} = 0.23 P_o. \quad (39)$$

The operation of the tapped interphase transformer is discussed in Section II-A. From Fig. 6(c), the voltampere rating of the interphase transformer can be written as

$$\mathrm{VA_{IR}} = \frac{V_{1,\mathrm{rms}} I_{o1,\mathrm{rms}} + V_{2,\mathrm{rms}} I_{o2,\mathrm{rms}} + V_{3,\mathrm{rms}} I_{o3,\mathrm{rms}}}{2}. \quad (40)$$

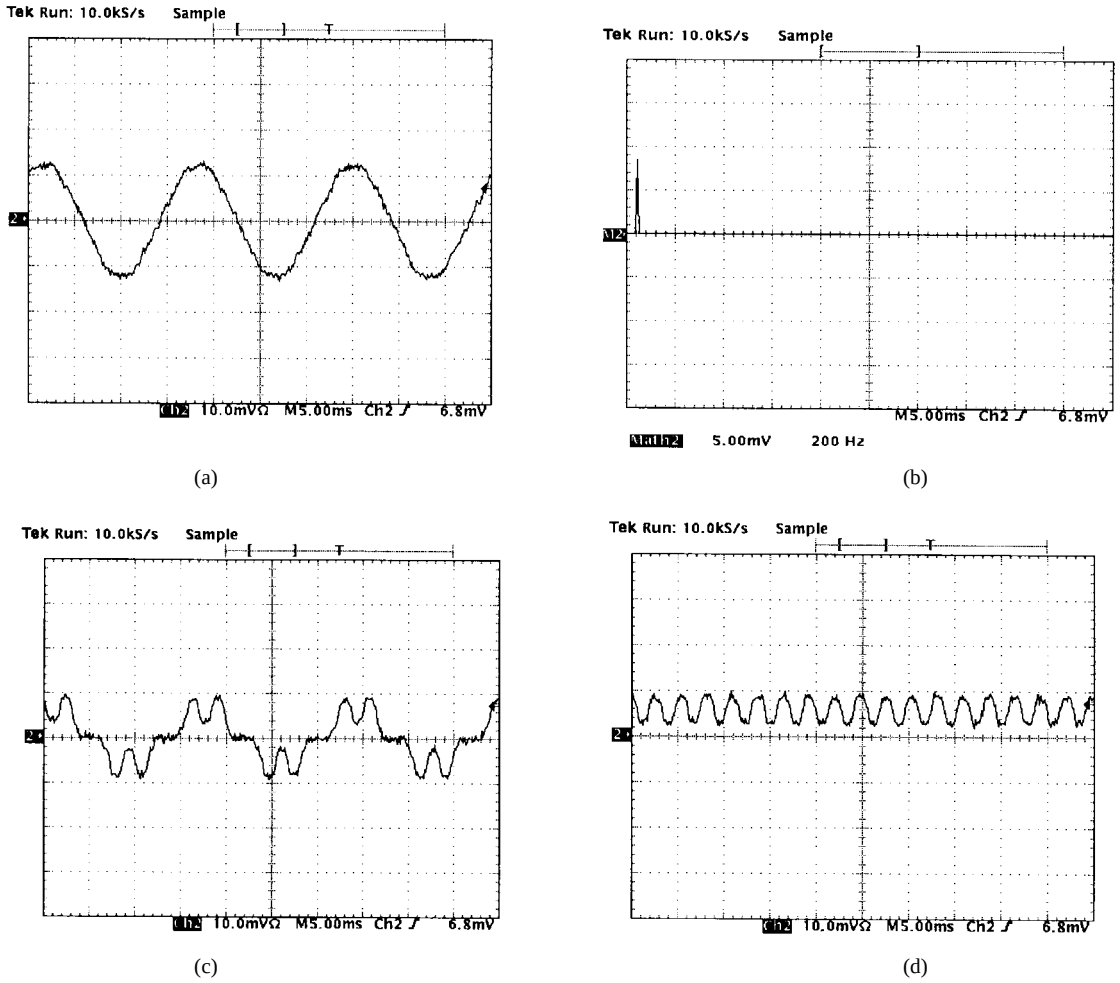

Fig. 11. Experimental results of the proposed 24-pulse system. (a) Input line current I_a (20 A/div). (b) Frequency spectrum of I_a (THD measured 3.4%). (c) Rectifier input current I_{a1} (20 A/div). (d) Rectifier output current I_{o1} (20 A/div).

From (30) and Fig. 8, we have rms currents of I_{o1}, I_{o2}, and I_{o3} as follows:

$$I_{o1,\mathrm{rms}} = I_{o2,\mathrm{rms}} = 0.567 I_o \quad \text{and} \quad I_{o3,\mathrm{rms}} = 0.232 I_o \tag{41}$$

where $I_{o3} = I_{o1} - I_{o2}$ [see Fig. 6(c)].

The rms voltage across the interphase transformer (Fig. 8) is given by

$$\begin{aligned} V_{m,\mathrm{rms}} &= \sqrt{\frac{1}{T}\int_0^T V_m^2 dt} \\ &= \sqrt{\frac{12}{\pi}\int_0^{\pi/12} \left(\left(\frac{\sqrt{2}}{1+\sqrt{3}}\right)(\sqrt{2}V_{LL})\sin(wt)\right)^2 dwt} \\ &= 0.0814 V_o \end{aligned} \tag{42}$$

and the voltages V_1, V_2, and V_3 can be written in terms of the voltage across the interphase transformer V_m as

$$\frac{V_1}{V_m} = \frac{V_2}{V_m} = \frac{(N_o - 2N_t)/2}{N_o} = 0.2543 \tag{43}$$

$$\frac{V_3}{V_m} = \frac{2N_t}{N_o} = 0.4914. \tag{44}$$

Therefore, the rms voltages of V_1, V_2, and V_3 are given by

$$V_{1,\mathrm{rms}} = V_{2,\mathrm{rms}} = 0.2543 V_{m,\mathrm{rms}} = 0.021 V_o \tag{45}$$

$$V_{3,\mathrm{rms}} = 0.4914 V_{m,\mathrm{rms}} = 0.04 V_o. \tag{46}$$

Substituting (41), (45), and (46) in (40), the voltampere rating of the interphase transformer is given by

$$\mathrm{VA}_{\mathrm{IR}} = 0.0165 P_o. \tag{47}$$

The lowest frequency component of the voltage (V_m) across the interphase transformer (Fig. 8) is 360 Hz; this results in smaller size, weight, and volume.

IV. Simulation Results

Schemes 1 and 2 of the proposed 24-pulse approach are simulated on SABER and the results are presented in this section. Fig. 10(g) shows the voltage across the interphase transformer. Fig. 10(f) shows the voltage across the ZSBT depicting tripplen components. The rectifier output current I_{o1} is shown in Fig. 10(d). Notice the current is modulated, due to the action of tapped interphase transformer and the alternative conduction of diodes D_p and D_q, and the currents I_{o1} and I_{o2} are equal. Fig. 10(c) shows the rectifier I input current

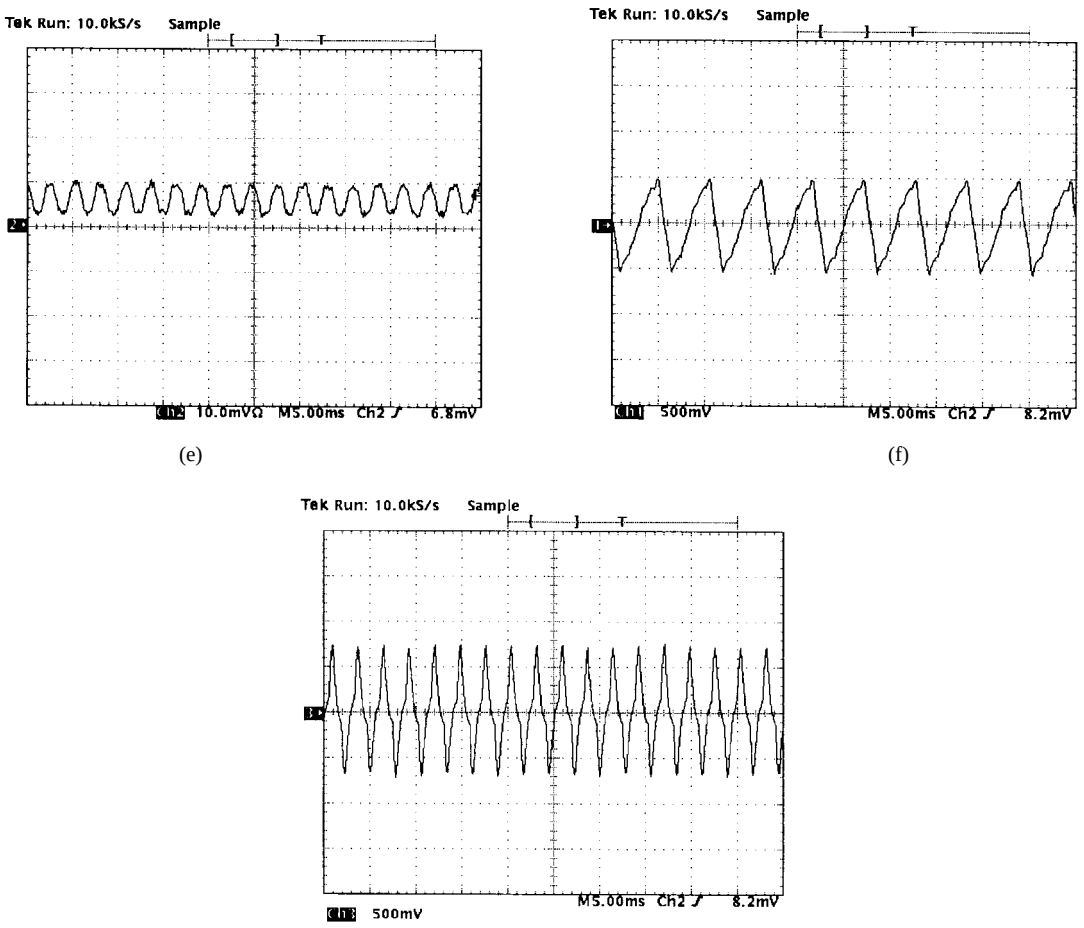

Fig. 11. (*Continued.*) Experimental results of the proposed 24-pulse system. (e) Rectifier output current I_{o2} (20 A/div). (f) Voltage across the ZSBT (50 V/div). (g) Voltage across the interphase transformer (25 V/div).

I_{a1}. Fig. 10(a) and (b) show input line current I_a and its frequency spectrum, respectively. Thus, Fig. 10(a) demonstrates 24-pulse operation with the fifth, seventh, eleventh, thirteenth, seventeenth, and nineteenth harmonics eliminated in the input line currents.

V. Experimental Results

A 208-V 10-kVA 24-pulse rectifier system, as shown in Fig. 6, has been constructed in the laboratory and is connected to supply a bank of dc-link capacitors. A resistive load bank is then used to load the dc link and to simulate an inverter-fed ac-drive load. The proposed system was connected in a 24–pulse configuration, and the results are discussed in this section.

Fig. 11(a)–(g) show the proposed system connected in a 24-pulse operating mode with the two additional diodes and the tapped interphase transformer (Fig. 6). Fig. 11(f) shows the V_{ZSBT1} voltage which is essentially zero sequence. Fig. 11(g) shows the voltage across interphase transformer V_m. Fig. 11(d) and (e) show the two rectifier input currents I_{o1} and I_{o2}, respectively. It is clear that the two rectifier output currents are automatically modulated by the action of the tapped interphase transformer and the two additional diodes D_p and D_q. Fig. 11(a) shows the resulting input current at half load; input current THD of 3.4% was recorded. It is clear that the proposed 24-pulse system exhibits superior performance and clean input power characteristics.

VI. Conclusion

In this paper, two new 24-pulse diode rectifier systems have been proposed for high-power motor drives. In the proposed scheme 1, it has been shown that a conventional 12-pulse system can be transformed to a 24-pulse system by employing a tapped interphase transformer and, in scheme 2, a passive 24-pulse rectifier system has been shown with the use of a reduced voltampere autotransformer. The resulting systems exhibit clean power characteristics with the elimination of fifth, seventh, eleventh, thirteenth, seventeenth, and nineteenth harmonics in the input line currents and are low cost in nature. Analysis and simulation results verify the basic concept. Experimental results demonstrate the superiority of the proposed schemes 1 and 2.

References

[1] *IEEE Recommended Practices and Requirements for Harmonic Control in Electrical Power Systems*, IEEE Standard 519-1992, 1993.

[2] S. Miyairi *et al.*, "New method for reducing harmonics involved in input and output of rectifier with interphase transformer," *IEEE Trans. Ind. Applicat.*, vol. IA-22, pp. 790–797, Sept./Oct. 1986.

[3] G. Oliver *et al.*, "Novel transformer connection to improve current sharing on high current DC rectifiers," in *Proc. 1993 IEEE-IAS Conf.*, pp. 986–992.
[4] P. W. Hammond, "Power quality for medium voltage AC drives," presented at the IEEE Petroleum and Chemical Industry Tech. Conf., Denver, CO, Sept. 1995.
[5] G. Seguier, *Power Electronic Converters AC/DC Conversions*. New York: McGraw-Hill, 1986.
[6] J. Schaefer, *Rectifier Circuits: Theory and Design*. New York: Wiley, 1965.
[7] R. E. Tarter, *Principles of Solid-State Power Conversion*. Indianapolis, IN: Sams, 1985, pp. 166–168.
[8] P. Enjeti, P. D. Ziogas, and J. F. Lindsay, "Programmed PWM technique to eliminate harmonics: A critical evaluation," *IEEE Trans. Ind. Applicat.*, vol. 26, pp. 302–316, Mar./Apr. 1990.
[9] D. A. Paice, *Power Electronic Converter Harmonics—Multi-Pulse Methods for Clean Power*. Piscataway, NJ: IEEE Press, 1995.
[10] S. Choi, P. Enjeti, and H. Lee, "A new reduced kVA multi-pulse diode rectifier front end for high power AC motor drives draws near sinusoidal input currents," in *Proc. Int. Conf. Power Electronics*, Seoul, Korea, Oct. 1995, pp. 110–115.
[11] S. Choi, P. Enjeti, and I. Pitel, "New polyphase transformer arrangements with reduced kVA capacities for harmonic current reduction in rectifier type utility interface," *IEEE Trans. Power Electron.*, vol. 11, pp. 680–690, Sept. 1996.

Sewan Choi (S'92-M'92) was born in Seoul, Korea, on March 3, 1963. He received the B.S. degree in electronic engineering from Inha University, Incheon, Korea, in 1985 and the M.S. and Ph.D. degrees in electrical engineering from Texas A&M University, College Station, TX, in 1992 and 1995, respectively.

From 1985 to 1990, he was with Daewoo Heavy Industries as a research engineer. From 1996 to 1997, he was a Principal Research Engineer at Samsung Electro-Mechanics Company, Ltd., Suwon, Korea. He is currently a full-time Instructor in the Department of Control and Instrumentation Engineering, Seoul National Polytechnic University, Seoul, Korea. His research interests include clean power utility interface, active power factor correction, and microprocessor control of power converters.

Bang Sup Lee (S'95) was born in Daejeon, Korea, in 1964. He received the B.S. degree in electrical engineering from Choongnam National University, Daejeon, Korea, in 1987 and the M.S. degree in electrical engineering from Seoul National University, Seoul, Korea, in 1989. He is currently working toward the Ph.D. degree at Texas A&M University, College Station, TX.

In 1989, he joined the Central Research and Development Center, Daewoo Heavy Industries, where he remained until 1994. His current research interests are in active power filter development, advance power converters, power quality issues, and adjustable-speed ac drives.

Mr. Lee was the recipient of the IEEE Industry Applications Society Third Best Paper Award in 1996.

Prasad N. Enjeti (S'86–M'88–SM'95) received the B.E. degree from Osmania University, Hyderabad, India, in 1980, the M.Tech. degree from the Indian Institute of Technology, Kanpur, India, in 1982, and the Ph.D. degree from Concordia University, Montreal, P.Q., Canada, in 1987, all in electrical engineering.

In 1987, he joined the Electrical Engineering Department, Texas A&M University, College Station, TX, where he is currently an Associate Professor. In 1996, he established the Power Electronics/Power Quality Laboratory at Texas A&M University. He is actively involved in many projects in industry and is engaged in teaching, research, and consulting in the areas of power electronics, power quality, and clean power utility interface issues. His primary research interests are advance converters for power supplies and motor drives, power quality issues and active power filter development, utility interface issues and "clean" power converter designs, and electronic ballasts for fluorescent HID lamps.

Dr. Enjeti is Transactions Editor for the Industrial Power Converter Committee (IPCC) of the IEEE Industry Applications Society (IAS) and an Associate Editor for the IEEE TRANSACTIONS ON POWER ELECTRONICS. He was the recipient of the IEEE-IAS Second and Third Best Paper Awards in 1993 and 1996, respectively, and the Second Best Transactions Paper Award published in mid-year 1994–mid-year 1995 in the IEEE TRANSACTIONS ON INDUSTRY APPLICATIONS. He is a Registered Professional Engineer in the State of Texas.